THE ASTROPHYSICAL JOURNAL, 464:684–689, 1996 June 20

LINE PROFILES FROM RELATIVISTIC ECCENTRIC RINGS

G. BAO,[1,2,3,4] P. HADRAVA,[5,6] AND E. ØSTGAARD[1,7]

Received 1995 June 5; accepted 1996 January 5

ABSTRACT

We find the existence of closed stationary precessing rings in general relativity, which are composed of particles moving on eccentric orbits around a central black hole. Emission-line profiles radiated by these eccentric rings in a Schwarzschild background are calculated by using a fully relativistic approach. The work is complementary to the recent paper by Eracleous et al., in which line profiles from an eccentric accretion disk are calculated under the weak field approximation, and the results presented in the present paper can be applied directly to some astrophysical systems. It is shown that both the line intensity and the profile from an eccentric ring are sensitive to a number of parameters, i.e., the eccentricity, the semimajor axis, the inclination, and the instantaneous longitude of periastron. Noticeably, the profiles show a large variety. In some cases, they have double peaks within the blue or red peak being higher, and in other cases, they show multiple peaks. These could have impact on the understanding of X-ray emission lines from active galactic nuclei and from X-ray binaries.

Subject headings: accretion, accretion disks — black hole physics — galaxies: active — line: profiles

1. INTRODUCTION

Accretion disks around black holes is currently the most plausible explanation of highly luminous objects such as active galactic nuclei (AGNs) and X-ray binaries. In spite of theoretical predictions, there is limited observational evidence for the existence of accretion disks. One of the information sources in favor of the disk model is the profiles of emission lines from accretion disks orbiting around compact objects, e.g., a black hole or a neutron star. It is well known that emission-line profiles from a relativistic accretion disk with zero eccentricity (a circular accretion disk) are characterized by double horns, with the blue horn being always stronger than the red one. The blue horn is attributed to emitting matter of the disk approaching the observer, whereas the red horn is caused by the matter receding from the observer. If the disk is in the close vicinity of a black hole, and if its inclination is larger than 80°, then the resulting profiles from the disk will show extra peaks between the two horns due to gravitational lensing of the light from the region behind the black hole relative to the distant observer.

Although some of the optical line profiles from (about 12) AGNs have been well fitted by the profiles resulting from relativistic accretion disks with zero eccentricities (see, e.g., Halpern 1990), there are still a considerable number of AGNs with optical line profiles quite different from those resulting from a circular disk. A line profile analysis for 61 (mostly radio-quiet) AGNs presented by Sulentic (1989) and Sulentic et al. (1990) shows a "stochastic" distribution of profiles and asymmetries. In their sample, the authors found no double-peaked emission-line profiles predicted by circular disk models. A similar result was obtained by Boroson & Green (1992) in their analysis of 87 PG quasars. Many disklike optical emission lines were found by Eracleous & Halpern (1994) in their sample of radio-loud AGNs. However, a large diversity of emission-line profiles is observed also.

Motivated by observational facts, Eracleous et al. (1995) recently investigated model line profiles from eccentric accretion disks and discovered that some of the observed profiles can be well fitted by their results. Two possible mechanisms have been proposed for the formation of an eccentric accretion disk, i.e., the disk is eccentric due to the presence of a companion of the central body (as in the case of mass exchange in binaries; see, e.g., Kříž & Harmanec 1975, Hensler 1985, Whitehurst 1988, Syer & Clarke 1992), or it is due to debris released from the tidal disruption of a star by the supermassive black hole in the active nucleus (see, e.g., Eracleous et al. 1995). A recent work by Lyubarskij, Postnov, & Prokhorov (1994) has shown that for any reasonable viscosity law, a nonrelativistic stationary eccentric accretion disk is possible, with all streamlines having the same eccentricity. However, the generalization of their results to the relativistic case can be problematic in the general-relativistic pericenter advance, which is dependent on the semimajor axis. In the discussion of their results, Eracleous et al. (1995) concluded that *the inner part of the disk can circularize due to differential precession before the outer part precesses by a significant amount*, and they limited the validity of their results in the cases in which *the inner and outer pericenter distances differ by less than a factor of 2.*

In our previous paper (Bao, Hadrava, & Østgaard 1994a, hereafter Paper I), we investigated light curves originating from emitting blobs moving on eccentric orbits in the strong-field region of the accretion disk. Because of the above-mentioned problems, we limited our subsequent study (Bao, Hadrava, & Østgaard 1994b, hereafter Paper II) of line profiles to the case of zero eccentricity of the disk. Here we will show that a stationary closed ring can exist also in a strong field, and its line profiles are calculated using a fully relativistic approach.

[1] Physics Institute, University of Trondheim, AVH, N-7055 Dragvoll, Norway.
[2] INFN Section of Padova, Department of Physics, University of Padua, Via Marzolo 8, 35131 Padua, Italy.
[3] Department of Physics and Astronomy, Georgia State University, Atlanta, GA 30303.
[4] bao@chara.gsu.edu
[5] Astronomical Institute of the Academy of Sciences of the Czech Republic, CZ-251 65 Ondřejov, Czech Republic.
[6] had@sunstel.asu.cas.cz.
[7] erlend.oestgaard@avh.unit.no.

The weak field approximation by Eracleous et al. (1995) would be sufficient in some cases; for example, if the inclination of the disk were not very high, and the emitting region were not very close to the central black hole. However, in the case of, for example, the X-ray emission iron line which is believed to originate from the region inside $100r_s$ (where r_s is the Schwarzschild radius $r_s = 2GM/c^2$), the approximation can be inaccurate. Also, X-ray lines from AGNs and from X-ray binaries can now be resolved by the new generation of satellites, such as the Japanese X-ray satellite *ASCA*; a fully relativistic investigation should therefore be carried out.

In the following section, we use the formulae of test-particle motion on eccentric orbits to construct a closed precessing ring. In § 3, the photon motion in Schwarzschild spacetime and a scheme for calculating the line profile are reviewed, and the results are presented. In the last section, we summarize the results and conclude with relevant discussions, especially on their astrophysical applications.

2. THE GEOMETRY AND DYNAMICS OF AN ECCENTRIC RING

The technique for calculating the motion of an individual emitting blob of matter (approximated by a test particle) on a relativistic eccentric orbit around a Schwarzschild black hole has already been presented in Paper I. It is well known that the orbit is not closed; instead, it spans an azimuthal angle

$$\varphi T = 4\frac{a^{1/2}(1-e^2)^{1/2}}{\Delta(\pi)}F(k)\,, \tag{1}$$

in one anomalistic orbit lasting the Schwarzschild coordinate time

$$T = 2C_1\left\{-\frac{1}{\Delta(\pi)}F(k) + C_2\,\Delta(\pi)E(k) + \frac{2}{a(1-e)\Delta(\pi)}\left[(a+3+4C_2)\Pi\left(C_3,\frac{\pi}{2},k\right) + \frac{4}{a(1+e)-2}\Pi\left(C_4,\frac{\pi}{2},k\right)\right]\right\}, \tag{2}$$

where $F(k)$, $E(k)$, and $\Pi(n, \pi/2, k)$ are the complete elliptic integrals of the first, second, and third kind, respectively (see eqs. [A7] and [A11] of Paper I). To understand, in principle, the existence of a closed stationary ring composed of particles moving on such an eccentric orbit, we transform the "inertial" Schwarzschild coordinates to a uniformly rotating coordinate system (with angular velocity ω_p), i.e.,

$$\varphi' = \varphi - \omega_p t = \varphi - \frac{\varphi_T - 2\pi}{t}t\,, \tag{3}$$

which corotates with the precession of a "pivoting" test particle with chosen semimajor axis a and eccentricity e. We will then arrive at a closed orbit, and a continuous set of particles launched on the same orbit with constant time delay will form an infinitesimally narrow, but closed ring, which is stationary. An example of such rings is given in Figure 1. Note the remarkable deviation from the Newtonian ellipse at the apocenter. This is caused by the difference between the angular velocity of each

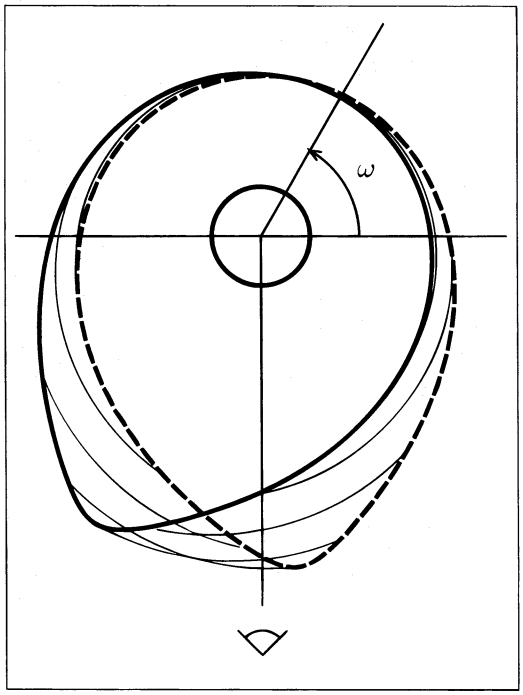

FIG. 1.—Shape of the eccentric ring with semimajor axis $a = 10m$ and eccentricity $e = 0.35$, drawn for Schwarzschild coordinates r, φ, taken as polar coordinates. The Schwarzschild radius is given by the central circle; the line of sights points down. The position of the ring with $\omega = 60°$ (marked by the arrow) is plotted by the thick solid line. Trajectories of eight particles (equally spaced in the period of their orbital motion) are drawn by thin lines. These trajectories initiate from the solid ring and end at the dashed ring wih ω increased by the precession.

particle (which has its smallest value here) and the precession (which is dominated by the pericenter passage). The particle motion can even be retrograde with respect to the corotating system for large eccentricities, and the corresponding orbit could be eight-shaped. However, such solutions are meaningless for gaseous rings. Following the method of a multiparticle cloud (Hadrava 1983), it is clear that a stable eccentric ring with nonzero dimensions will result if extended gaseous blobs instead of dimensionless particles are launched on the same orbit. The streamlines inside such a disk, which must be supported by the gradient of pressure, cannot be obtained as trajectories of noninteracting test particles, but they can be solved from hydrodynamic equations. Because of a large number of free parameters involved in such configurations, we shall postpone this problem to a following study. Here we shall give some examples of line profiles radiated by the narrow rings described above.

3. CALCULATIONS OF THE LINE PROFILES RADIATED BY AN ECCENTRIC RING

The technique for line-profile integrations has already been described in Paper II. Here we only give a brief summary with a few comments.

Assuming the observer to be at rest at infinity in the direction $\vartheta = i$ (the inclination) and $\varphi = 0$, the trajectory of the observable photons emitted by the orbiting source at $r = r_s$ and $\varphi = \varphi_s$ can be found, solving for their impact parameter B (see Bao 1992). Note also that the higher order images could, in principle, be observable for an infinitesimally narrow ring. These can be taken into account as described in our Paper II. However, we shall not include them into the present calculations, in order to facilitate the understanding of the features caused by the eccentricity of the ring.

The time delay caused by the light travel time can be calculated straightforwardly for a known photon trajectory. It could influence the observable effects for rings with the fast precession (for which the instantaneous line profile would be a mixture of those corresponding to different longitudes of periastron with light time neglected). However, as one can see from Table 1 where the delay Δt between photons emitted at pericenter and apocenter for $\omega = 90°$ (which is the maximum) is given, it is valid for sufficiently large orbits that $\Delta t \ll T \ll T_p$, where $T_p = 2\pi/\omega_p$. Thus, we shall neglect this effect here.

For a known photo trajectory and the source four-velocity, the redshift and gravity lensing effect can be calculated. For the sake of simplicity, we assume that line photons escape freely to us once emitted. This means that the corona around the emitting matter is optically thin. Here we consider only the Doppler broadening of lines due to the orbital motion of the ring, and we neglect such mechanisms as thermal broadening and Compton broadening (i.e., the emitted line profile is given by a δ-function). Once the emissivity of each part of the ring is known, its contribution to the observed flux can be calculated and integrated to the particular bin of the line profile (see Paper II). In the present calculations, we suppose the ring to be geometrically thin and consequently its radiation to be cosine dependent in its proper frame. Moreover, we assume its luminosity per unit mass to be constant in its proper time. This need not be the case in a real eccentric disk, which can be heated to temperatures varying along the orbit either due to hydrodynamic effects or due to reprocessing of external hard X-ray photons. Because we use the true anomaly v as the independent variable for the sampling of the motion of the ring, the contribution of each ring element to the total radiated energy is inversely proportional to the (proper) time derivative

$$\dot{v} = \left\{ \frac{a(1-e^2)[(a(1-e^2)-4)r - 2a(1-e^2)]}{r^5[a(1-e^2)-3-e^2]} \right\}^{1/2}, \tag{4}$$

which can be found from the equations of motion (see Paper I).

To illustrate the influence of the eccentricity on the line profile, several examples are given in Figures 2 and 3. For small eccentricities, the lines are basically double-horned (see the first two columns in Fig. 2) due to the fact that each ring element spends most of its orbital period close to the extremes of radial velocity. The blue peak is higher due to the Doppler enhancement. However, for higher eccentricities and periastron longitude $\omega \sim 180°$, the intensity ratio of the blue and red peak can be reversed (see the bottom of the third column in Fig. 2) due to the faster motion in the blueshifted periastron region.

Unlike the Newtonian case, the redshift g can have a secondary minimum and maximum as a function of the position in the ring (see Fig. 3, which corresponds to the parameters of the line profile shown at the bottom right of Fig. 2). This is caused by a more complicated goemetry and dynamics of the ring compared to the simple motion of an individual blob of matter. As a consequence, the line profile can have additional peaks at the corresponding values of g (see the fourth column of Fig. 2 and also the top of the column, where the same effect is less pronounced). These features are additional to the lensing enhancement known already from circular disks (Bao & Stuchlík 1992; Matt et al. 1992) and to the contribution of the higher order images (Paper II).

TABLE 1

LIGHT TRAVEL TIME Δt (FOR $i = 89.°9$ AND $\omega = 90°$) AND ANOMALISTIC (T), AND PRECESSION (T_p) PERIODS FOR SEVERAL ECCENTRIC ORBITS

	$e = 0.01$			$e = 0.5$		
a	Δt	T	T_p	Δt	T	T_p
100.....	209.6	6480.6	206227.7	210.8	6482.9	152133.4
50.....	108.5	2368.1	35873.9	109.7	2371.8	25979.0
20.....	47.1	671.7	3440.1	48.6	681.5	2317.9
10.....	26.1	314.2	540.5	28.1	256.8	382.3

NOTE.—All values in units of mass of the central black hole.

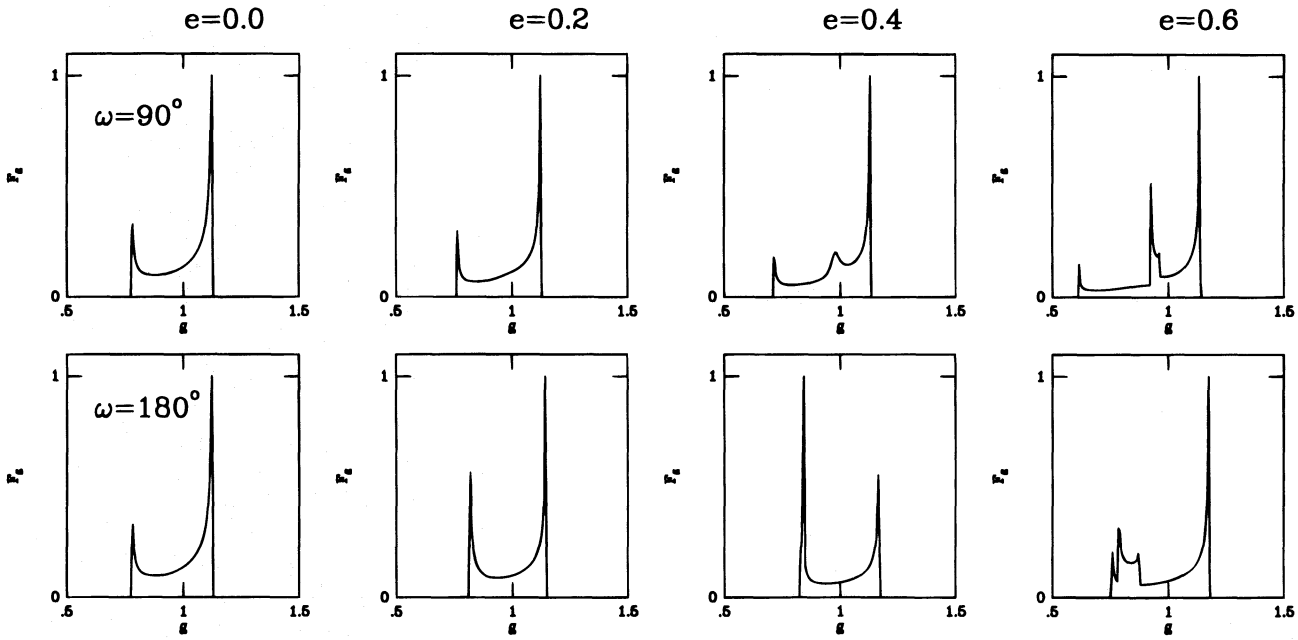

FIG. 2.—Line profiles from eccentric rings with $a = 20m$ and eccentricities $e = 0$, 0.2, 0.4, 0.6 (corresponding to each column) seen under inclination $i = 50°$ and different longitudes of the periastron (each row).

It is interesting that when the periastron longitude $\omega = 90°$ and 270°, apart from the peaks known as the blue and red peaks, there is another distinctive peak in between (see Fig. 2). Especially when $\omega = 90°$, the peak is close to the zero shift (i.e., $g = 1$). This is because the zero shift phase of the ring has a large contribution.

In general, the eccentric rings yield a large variety of line profiles, and the ring precession is responsible for the variability of profiles (see Fig. 4).

4. CONCLUSION AND DISCUSSION

Emission-line profiles with various parameters from a closed relativistic eccentric ring are presented. It is shown that once the semimajor axis and the eccentricity of a ring are given, the shape of the profiles is most sensitive to the orientation (the longitude) at which an observer looks. In principle, the resulting profiles can be single-peaked lines either blueshifted or redshifted; they can also be double-peaked with either the blue or the red peak being higher, depending on the orientation. They can even be triple-peaked, with the central peak close to the rest energy of the line (Fig. 4). It is obvious that the line intensities are also affected by the inclination of the ring.

It should be mentioned that although we study only line profiles from a narrow eccentric ring, it can be expected that the profiles from an extended ring, i.e., from a disk, should not be dramatically different, and that the results should be generalizable to some realistic astrophysical situations. A direct application of our results is the case of the released debris in the process of disruption of a star after a tidal encounter with a supermassive black hole (Eracleous et al. 1995), where an eccentric emission ring can last a long time, say a decade. The orbit of the post-disruption debris in a strong tidal encounter is studied by Laguna et al. (1993), who show that the trajectories of the debris form a crescentlike shape centered on the black hole. Detailed evolution of the debris is studied by Kochanek (1994). It is shown that during the first several orbits, the trajectories of debris are insensitive to the ambient medium. The debris broadens out into a circular disk only after a viscous

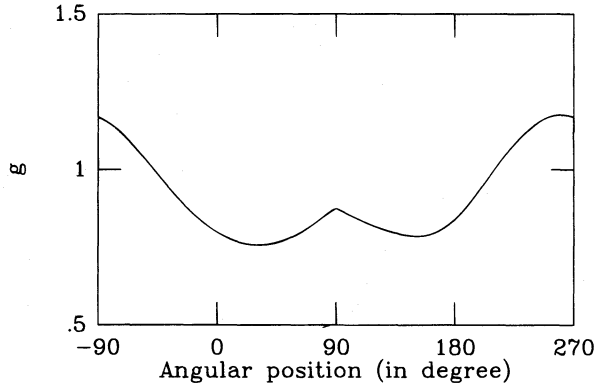

FIG. 3.—Dependence of the redshift on the position in the ring, with parameters $a = 20m$, $e = 0.6$, $\omega = 180°$, and $i = 50°$

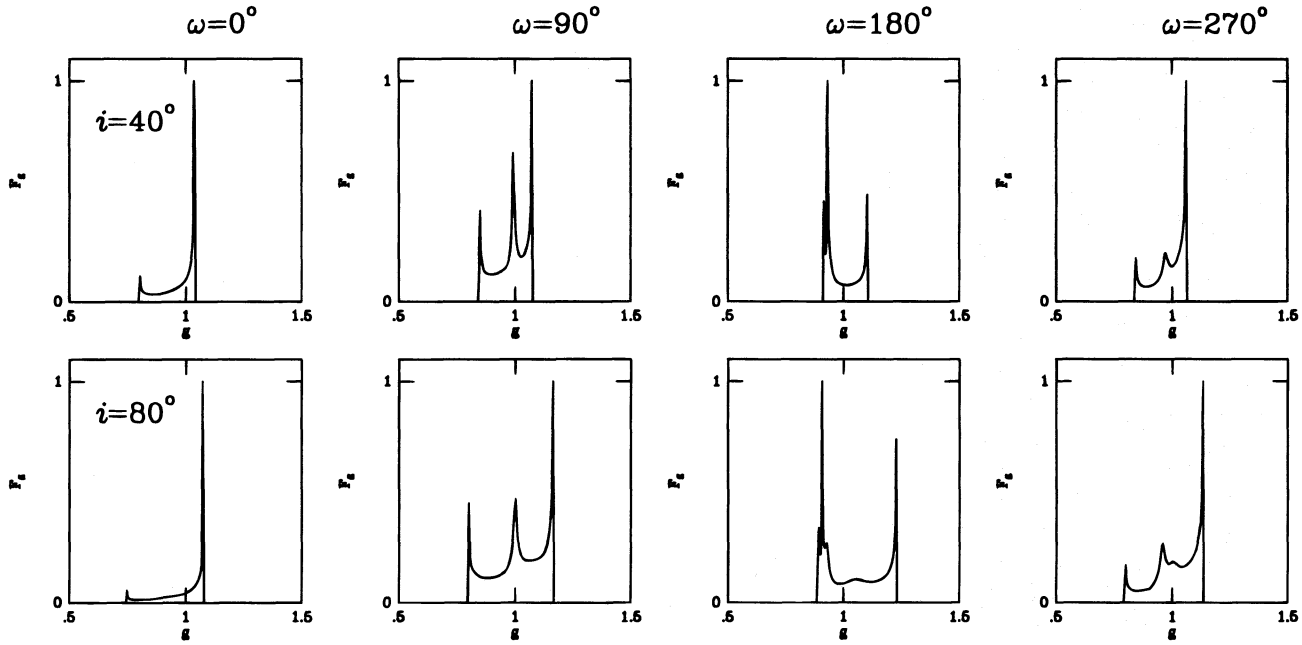

FIG. 4.—Line profiles from an eccentric ring with $a = 50m$ and $e = 0.5$, seen under inclinations $i = 40°$ and $i = 80°$ (each row), with different longitudes of periastron ω (corresponding to each column).

time, which is of order of 50 yr (Syer & Clarke 1992; Eracleous et al. 1995). It must be noted that in some specific situation fast general relativistic differential precession in the innermost area around the black hole would circularize the disk quickly and make the results of the present paper inapplicable. Such circularization is indicated by numerical hydrodynamic models (Syer & Clark 1992; Kojima 1995); however, it is obvious that this result is dependent on the initial conditions chosen.

Features of emission lines of active galactic nuclei (AGNs) and Galactic black hole candidates are the important signatures of the accreting matter around the central black hole. Therefore, the study of emission lines would eventually lead to the mapping of the innermost region of accretion disks. There have been extensive studies of lines from circular relativistic accretion disks (Fabian et al. 1989; Stella 1990; Laor 1991; Kojima 1991; Chen & Eardley 1991; Bao 1993; Matt, Perola, & Stella 1993; Paper II; Karas, Lanza, & Vokrouhlicky 1995, and references therein), which has enhanced our understanding of emission lines from both AGNs and X-ray binaries. Broad double-horned line profiles have been resolved in the optical spectra of several AGNs, and the profiles have been well fitted with those from circular accretion disks around black holes; for example, the Balmer lines of Arp 102B, 3C 332 (Halpern 1990; Chen, Halpern, & Filippenko 1989). The big "UV bump" in the ultraviolet emission of Seyfert 1 galaxies or quasars, and the double-peaked optical lines, constitute a proof of an accretion disk extending at least up to $10^3 r_s$. The iron line at 6–7 keV, originating from the innermost part of an accretion disk, has also been detected in the X-ray spectra of some AGNs (>90% of Seyfert galaxies) and Galactic black hole candidates (Barr, White, & Page 1985; White et al. 1986; Pounds et al. 1989; Nandra et al. 1989; Pounds et al. 1990). The discovery of high-energy spectra flattenings (the "hard tail" above ~ 10 keV) together with the iron K fluorescence line are currently interpreted as due to cold "reflecting" matter ($< 10^6$ K) around a black hole. Recently, the disklike profile of the Kα line was resolved by the *ASCA* satellite in the AGN MCG −6-30-15 (Tanaka et al. 1995). It is suggested that the line originates from a narrow region close to a central black hole. If this phenomenon is common in AGNs, then our results on eccentric rings could help to analyze the fine structure of the line profiles. Despite the spectral resolution and the signal-to-noise ratio of the present observations still being below the desirable limit, it indicates that the features (discussed above) in the fine structure of line profiles formed in the innermost part of the accretion disk will soon make a powerful observational test of AGN models.

Despite some of the good fittings of optical lines, most of the observed profiles are contradictory to the resulting line profiles from a circular disk model which shows a double-peaked line with the blue peak always being higher than the red one. An eccentric accretion disk seems, in some cases, plausible for the explanation of the observed line profiles. Physically, an eccentric disk is also realistic. For example, it may be formed during the mass transfer in binary systems.

In addition, as many authors have claimed, one still cannot exclude the possibility that the observed emission lines are caused by jets, in which case each of two jets of a source produces a shifted single peak, and the combined line profiles have double peaks or twin shoulders (Hadrava & Zentsova 1988). But this mechanism is not likely to produce a triple or even more peaked profile. Another possibility for formation of double-peaked line profiles in AGNs could be their binary nature analogous to Galactic double-line binaries, but with orbital periods much longer than the contemporary period of their observations (see Halpern & Filippenko 1988, and references therein). Also there might exist such a mechanism as spiral shocks (Chakrabarti & Wiita 1994) producing various profiles.

To tell the difference of line profiles resulting from different mechanisms, a systematic study of the profiles from different models is obviously needed.

We thank Mike Eracleous for his constructive comments. This work has been supported by the Norwegian Research Council and Czech grants no. 303401 and 202/93/0503.

REFERENCES

Bao, G. 1992, A&A, 257, 594
———. 1993, ApJ, 409, L41
Bao, G., Hadrava, P., & Østgaard, E. 1994a, ApJ, 425, 63 (Paper I)
———. 1994b, ApJ, 435, 55 (Paper II)
Bao, G., & Stuchlík, Z. 1992, ApJ, 400, 163
Barr, P., White, N. E., & Page, C. G. 1985, MNRAS, 216, 65p
Boroson, T. A., & Green, R. F. 1992, ApJS, 80, 109
Chakrabarti, S. K., & Wiita, P. J. 1994, ApJ, 434, 518
Chen, K., & Eardley, D. 1991, ApJ, 382, 125
Chen, K., Halpern, J. P., & Filippenko, A. V. 1989, ApJ, 339, 742
Eracleous, M., & Halpern, J. P. 1994, ApJS, 90, 1
Eracleous, M., Livio, M., Halpern, J. P., & Storchi-Bergmann, T. 1995, ApJ, 438, 610
Fabian, A. C., Rees, M., Stella, L., & White, N. E. 1989, MNRAS, 238, 729
Hadrava, P. 1983, Bull. Astron. Inst. Czechosl., 34, 234
Hadrava, P., & Zentsova, A. S. 1988, Bull. Astron. Inst. Czechoslovakia, 39, 345
Halpern, J. P. 1990, ApJ, 365, L51
Halpern, J. P., & Filippenko, A. V. 1988, Nature, 331, 46
Hensler, G. 1985, A&A, 148, 423
Karas, V., Lanza, A., & Vokrouhlický, D. 1995, ApJ, 440, 108
Kochanek, C. 1994, ApJ, 422, 508
Kojima, Y. 1991, MNRAS, 250, 629
———. 1995, in 14th International Conference on General Relativity and Gravitation, in press
Kříž, S., & Harmanec, P. 1975, Bull. Astron. Inst. Czechoslovakia, 26, 65
Laguna, P., Miller, W. A., Zurek, W. H., & Davies, M. B. 1993, ApJ, 410, L83
Laor, A. 1991, ApJ, 376, 90
Lyubarskij, Yu. E., Postnov, K. A., & Prokhorov, M. E. 1994, MNRAS, 266, 583
Matt, G., Perola, G. C., Piro, L., & Stella, L. 1992, A&A, 257, 63
Matt, G., Perola, G. C., & Stella, L. 1993, A&A, 267, 643
Nandra, K., Pounds, K. A., Stewart, G. C., Fabian, A. C., & Rees, M. J. 1989, MNRAS, 236, 39P
Pounds, K. A., Nandra, K., Stewart, G. C., George, I. M., & Fabian, A. C. 1990, Nature, 344, 132
Pounds, K. A., Nandra, K., Stewart, G. C., George, I. M., & Leighly, K. 1989, MNRAS, 240, 769
Stella, L. 1990, Nature, 344, 747
Sulentic, J. W. 1989, ApJ, 343, 54
Sulentic, J. W., Calvani, M., Marziani, P., & Zheng, W. 1990, ApJ, 355, L15
Syer, D., & Clarke, C. J. 1992, MNRAS, 255, 92
Tanaka, Y., et al. 1995, Nature, 375, 659
White, N. E., Peacock, A., Hasinger, G., Mason, K. O., Manson, K. O., Manzo, G., Taylor, B. G., & Branduardi-Raymont, G. 1986, MNRAS, 218, 129
Whitehurst, R. 1988, MNRAS, 232, 35